IL-2 consumption by highly activated CD8 T cells induces regulatory T-cell dysfunction in patients with hemophagocytic lymphohistiocytosis

Stéphanie Humblet-Baron, MD, PhD,[a,b]* Dean Franckaert, MSc,[a,b]* James Dooley, MSc,[a,b] Simon Bornschein, MSc,[a,b] Bénédicte Cauwe, PhD,[a,b] Susann Schönefeldt, MSc,[a,b] Xavier Bossuyt, MD, PhD,[b,c] Patrick Matthys, PhD,[e] Frédéric Baron, MD, PhD,[f] Carine Wouters, MD, PhD,[c,d] and Adrian Liston, PhD[a,b]   *Leuven and Liege, Belgium*

Background: Hemophagocytic lymphohistiocytosis (HLH) is a severe inflammatory condition driven by excessive CD8^{+} T-cell activation. HLH occurs as both acquired and familial hemophagocytic lymphohistiocytosis (FHL) forms. In both conditions, a sterile or infectious trigger is required for disease initiation, which then becomes self-sustaining and life-threatening. Recent studies have attributed the key distal event to excessive IFN-γ production; however, the proximal events driving immune dysregulation have remained undefined.
Objective: We sought to investigate the role of regulatory T (Treg) cells in the pathophysiology of experimental FHL.
Methods: Because mutation in perforin is a common cause of FHL, we used an experimental FHL mouse model in which disease in perforin-deficient mice is triggered by lymphocytic choriomeningitis virus (LCMV). We assessed Treg and CD8^{+} T-cell homeostasis and activation during the changing systemic conditions in the mice. In addition, human blood samples were collected and analyzed during the HLH episode.
Results: We found no primary Treg cell defects in perforin-deficient mice. However, Treg cell numbers collapsed after LCMV inoculation. The collapse of Treg cell numbers in LCMV-triggered perforin-deficient, but not wild-type, mice was accompanied by the combination of lower IL-2 secretion by conventional CD4^{+} T cells, increased IL-2 consumption by activated CD8^{+} T cells, and secretion of competitive soluble CD25. Moreover low Treg cell numbers were observed in untreated patients experiencing HLH flares.
Conclusion: These results demonstrate that excessive CD8^{+} T-cell activation rewires the IL-2 homeostatic network away from Treg cell maintenance and toward feed-forward inflammation. These results also provide a potential mechanistic pathway for the progression of infectious inflammation to persistent inflammation in patients with HLH. (J Allergy Clin Immunol 2016;138:200-9.)

Hemophagocytic lymphohistiocytosis (HLH) is a severe inflammatory immune syndrome characterized by prolonged fever with hepatosplenomegaly, cytopenia, hepatitis, and neurologic manifestations.[1,2] The principal immunologic features of this syndrome are uncontrolled expansion of CD8^{+} cytotoxic T cells, activation of antigen-presenting cells/macrophages (histiocytes), natural killer cell dysfunction, and florid cytokine storm, including high amounts of IFN-γ and TNF-α. Clinical manifestations are a consequence of hypercytokinemia and infiltration by activated lymphocytes and histiocytes of the bone marrow, spleen, liver, and central nervous system.[1,2]

Familial hemophagocytic lymphohistiocytosis (FHL) is caused by genetic deficiency in the cytotoxic pathways of T and natural killer cells, with mutations in the genes encoding perforin *(Prf1)* or the perforin secretion components Munc13-4, Munc18-2, or Syntaxin 11 accounting for most cases.[2] A secondary form of acquired HLH can also arise after a broad variety of initiators, including infections, malignancies, or autoimmune diseases, with a specific condition called macrophage activation syndrome (MAS) mainly diagnosed in patients with systemic juvenile idiopathic arthritis.[1,2]

Despite progress in our understanding of HLH pathogenesis, treatment of HLH has remained unsatisfactory. In addition to treating the trigger event, current treatments for HLH are based on highly immunosuppressive drugs and chemotherapy, whereas allogeneic hematopoietic stem cell transplantation can be considered in patients with FHL and severe forms of HLH.[3]

Preclinical models for studying FHL have been developed using lymphocytic choriomeningitis virus (LCMV)–triggering inflammation in perforin-deficient mice.[4,5] These murine models recapitulate the key components of human disease, including life-threatening inflammation, cytopenia, cytokine storm, and

Abbreviations used
CTLA4: Cytotoxic T lymphocyte–associated antigen 4
  FHL: Familial hemophagocytic lymphohistiocytosis
Foxp3: Forkhead box protein 3
  HLH: Hemophagocytic lymphohistiocytosis
 IPEX: Immune dysregulation, polyendocrinopathy, enteropathy,
        X-linked
LCMV: Lymphocytic choriomeningitis virus
  MAS: Macrophage activation syndrome
  Prf1: Perforin gene
sCD25: Soluble CD25
STAT5: Signal transducer and activator of transcription 5
  Treg: Regulatory T

immune cell infiltration in different organs, including the liver and central nervous system. Specifically, these studies helped to uncover the pathophysiology of FHL, demonstrating that both CD8$^+$ T cells and IFN-γ are the principal terminal effectors of the disease. In addition, sustained antigen presentation has been reported to be essential to trigger CD8$^+$ activation,[6] and most patients with FHL have a history of viral infections acting as triggers. However, current models do not explain one of the most perplexing aspects of the clinical presentation of HLH, namely that some patients are given a diagnosis after the (presumably) viral trigger has been cleared, with self-perpetuating sterile inflammation developing. In addition, *in utero* FHL diseases have been described,[7,8] again indicating the capacity for the disease to be noncontingent on persistent infection. This observation indicates that we are currently still missing a key step in the pathogenesis of HLH, namely how excessive IFN-γ production and CD8$^+$ T-cell activation during a viral infection can continue and progress into a persistent hyperinflammatory state independent of viral burden. This process suggests that excessive CD8$^+$ T-cell activation might require additional proximal events to develop into the relentless inflammatory state of HLH.

One potential player in the pathogenic process of HLH might be regulatory T (Treg) cells.[9] Treg cells have a unique suppressive function in the immune system, a function imparted by the transcription factor forkhead box protein P3 (Foxp3). Mutations in *FOXP3* cause a fatal autoimmune and inflammatory disorder in both human subjects (immune dysregulation, polyendocrinopathy, enteropathy, X-linked [IPEX] syndrome) and mice (Scurfy mice). In addition, defects in Treg cell homeostasis promote autoimmunity and inflammation in patients with multiple other disorders,[10,11] demonstrating the vital role of Treg cells in preventing systemic inflammation. Here, we sought to determine whether Treg cells were involved in the malfunction of immune suppression that allows defective antiviral immunity to progress to fatal systemic inflammation in patients with FHL. Using LCMV-driven inflammation in perforin-deficient mice, we demonstrate that excessive activation of CD8$^+$ T cells during FHL creates an IL-2–limiting environment and reverses the IL-2 consumption hierarchy. These processes drive a collapse of the Treg cell population in both mice and patients and provide potential mechanistic explanation for the progression of infectious inflammation into the persistent systemic inflammation characteristic of HLH.

METHODS
Patients
Diagnostic data were obtained from patients with FHL/MAS during routine clinical care at UZ Leuven. Neonatal patients were excluded from analysis. Of the 7 patients identified during active FHL/MAS, 3 had not received any treatment related to an FHL/MAS episode at the time of the analysis, whereas 4 other patients had already started corticosteroids, cyclosporine treatment, or both. Written informed consent was obtained from each patient. The Ethics Committee of the University of Leuven and University Hospital approved the consent form and the current research study.

Mice
Perforin-deficient (C57BL/6-*Prf1*^{tm1Sdz}/J, Jackson Laboratory, Bar Harbor, Me) and C57BL/6 controls (Charles River, Wilmington, Mass) were analyzed at 8 to 12 weeks of age. Perforin-deficient mice were backcrossed to the *Cd127*$^{Cre/wt}$*Mcl1*$^{fl/wt}$ background[12,13] for use of the huCD4 reporter. Mice were maintained in specific pathogen-free facilities at the University of Leuven. All experiments were approved by the University of Leuven and the University of Liège Animal Ethics Committee.

Virus and infection
LCMV-Armstrong was produced and titrated, as previously described.[14] Mice were infected with 10^5 plaque-forming units of LCMV-Armstrong intraperitoneally on day 0 and were monitored and analyzed at day 10 after infection, unless otherwise specified. A subset of mice were administered murine IL-2/anti–IL-2 immune complex (1.5 μg/15 μg per mouse, JES6-1A12 clone; eBioscience, San Diego, Calif) intraperitoneally every other day starting on day 0 with LCMV injection.

Mouse blood analysis
Mouse blood samples were analyzed with the CELL-DYN 3700 (Abbott, Abbott Park, Ill) to determine red cell and platelet counts, as well as hematocrit and hemoglobin contents.

Flow cytometry
Single-cell suspensions were prepared from mouse spleens and pooled lymph nodes (cervical, inguinal, mesenteric, axillary, and brachial). For intracellular cytokine staining, lymphocytes were plated at 5 × 10^5 cells/well in 96-well tissue-culture plates in complete RPMI containing phorbol 12-myristate 13-acetate (50 ng/mL; Sigma-Aldrich, St Louis, Mo), ionomycin (250 ng/mL, Sigma-Aldrich), and monensin (1:1500; BD Bioscience, San Jose, Calif) for 4 hours at 37°C. All cells were fixed with BD Cytofix (BD Biosciences) or fixed and permeabilized with the eBioscience Foxp3 staining kit (eBioscience). For phospho–signal transducer and activator of transcription 5 (STAT5) staining, lymphocytes were plated at 5 × 10^6 cells/well in 96-well tissue-culture plates in complete RPMI containing murine IL-2 (100 ng/mL, eBioscience) and stimulated for 30 minutes before fixation with IC Fixation Buffer (eBioscience) and methanol. Anti-murine antibodies included anti-CD4 (RM4-5), anti-CD8a (53-6.7), anti-FoxP3 (FJK-16s), anti-CD25 (PC61.5), anti–cytotoxic T lymphocyte–associated antigen 4 (CTLA4; UC10-4B9), anti-CD69 (H1.2F3), anti-CD103 (2E7), anti-CD44 (IM7), anti-CD62L (MEL-14), anti-IL-2 (JES6-5H4), anti–IFN-γ (XMG1.2), and anti–phospho-STAT5 (SRBCZX) from eBioscience and anti-Ki67 (B56) from BD Biosciences. Anti-human CD4 staining was performed with BV-421 (OKT4; BioLegend, San Diego, Calif). Human peripheral blood was stained with anti-human antibodies, including anti-CD4 (5K3), anti-CD25 (2A3), and anti-CD127 (hIL-7R-M21). Data were collected on a BD FACSCanto II (BD Biosciences) and analyzed with FlowJo software for Mac, version 9.6 (TreeStar, Ashland, Ore).

CD8$^+$ *in vitro* stimulation
Purified CD8$^+$ T cells were isolated from spleens and lymph nodes of wild-type and IFN-γ–deficient mice (Jackson Laboratory) by using untouched
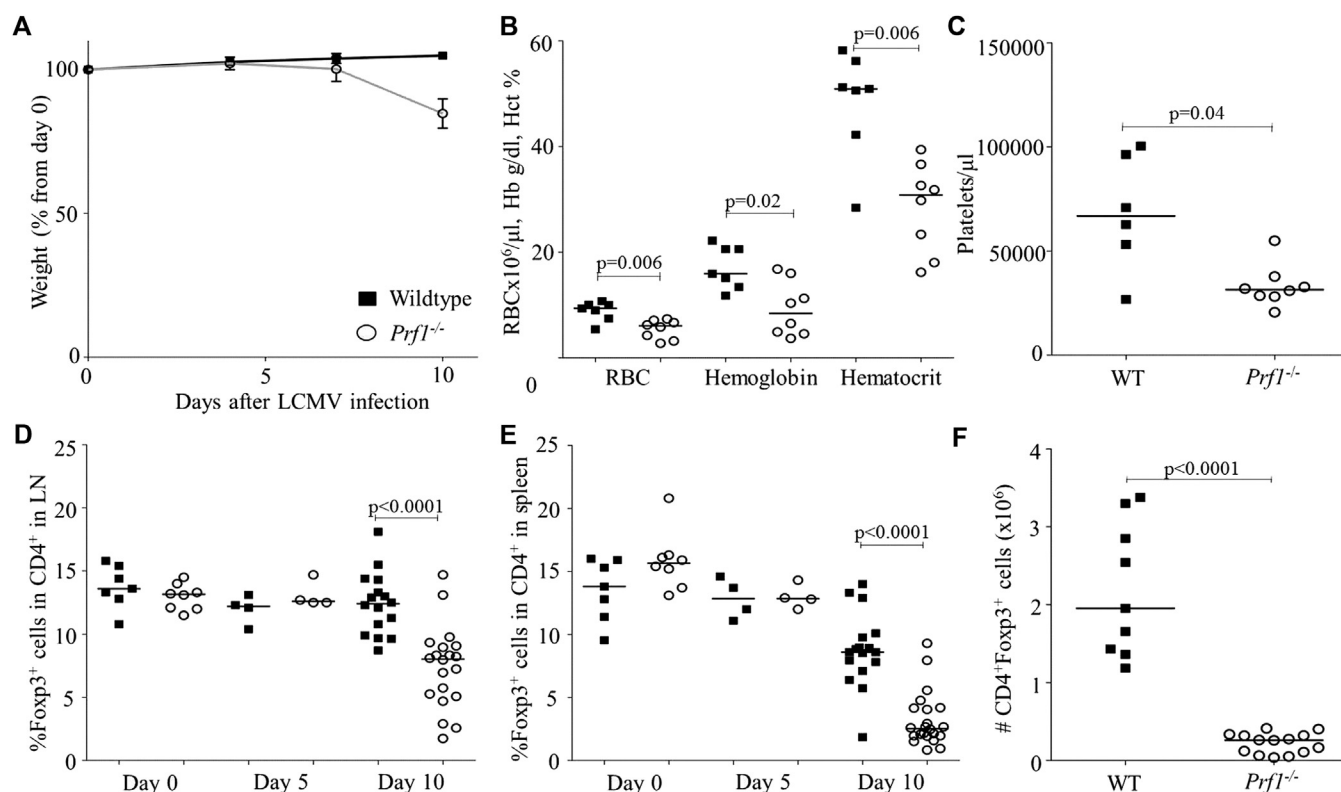
FIG 1. Treg cell collapse during LCMV-induced HLH. Wild-type mice and $Prf1^{-/-}$ mice were infected with LCMV-Armstrong. **A,** Mouse weight. **B,** Hemogram value with RBCs, hemoglobin, and hematocrit (day 10). **C,** Platelet level (day 10). **D-F,** Percentage of CD4$^+$Foxp3$^+$ Treg cells in lymph nodes (LN; Fig 1, *D*) and percentage (Fig 1, *E*) and numbers (Fig 1, *F*) in the spleen (day 10). Median and individual data points are shown. Fig 1, *A,* Representative of 7 experiments. Fig 1, *B-F,* Results pooled from 2 to 7 experiments.

CD8$^+$ magnetic isolation (STEMCELL Technologies, Vancouver, British Columbia, Canada). Cells were cultured in complete RPMI media and stimulated with phorbol 12-myristate 13-acetate (25 ng/mL, Sigma-Aldrich) and ionomycin (250 ng/mL, Sigma-Aldrich) or anti-CD3 (10 μg/mL, precoated overnight at 4°C; BD Biosciences) with or without additional IFN-γ (500 ng/mL, eBioscience) in addition to recombination-activating gene 2–deficient splenocytes. Supernatants and cells were harvested 48 hours later.

ELISA

Soluble CD25 (sCD25) titers in individual plasma samples and supernatants were determined by using a mouse IL-2Rα DuoSet ELISA (R&D Systems, Minneapolis, Minn), according to the manufacturer's protocol.

Statistical analyses

Single comparisons were analyzed by using the nonparametric Mann-Whitney *U* test. Spearman correlation was used for correlation tests. All statistical analyses were carried out with GraphPad Prism (version 5; GraphPad Software, La Jolla, Calif).

RESULTS

Defective Treg cell homeostasis during HLH

To determine the proximal cause of uncontrolled inflammation in patients with FHL, we investigated the properties of Treg cells, one of the key regulators of immune activation. Perforin knockout ($Prf1^{-/-}$) mice, with the same underlining genetic deficiency as patients with FHL, were used to assess Treg cell status. To investigate Treg cell homeostasis during inflammation in an FHL murine model, wild-type and $Prf1^{-/-}$ mice were treated with LCMV (Armstrong strain). After infection, wild-type mice experienced a transient immune activation with splenomegaly, whereas $Prf1^{-/-}$ mice had a terminal inflammatory disease that recapitulated the key aspects of FHL, including wasting, inflammatory anemia, and thrombocytopenia (Fig 1, *A-C*), as previously reported.[4,15] Disease was also associated with reduced splenic monocyte and increased neutrophil counts (see Fig E1 in this article's Online Repository at www.jacionline.org). In the absence of inflammation and at day 5 after infection, $Prf1^{-/-}$ mice had the same number of Treg cells as wild-type mice, as defined by Foxp3-expressing cells within CD4$^+$ T cells, indicating no primary defect in Treg cell homeostasis (Fig 1, *D* and *E*). However, 10 days after infection, the Treg cell population in wild-type mice infected with LCMV was reduced by approximately 40%, whereas perforin-deficient mice experience a collapse in Treg cell numbers, with an approximately 90% reduction in the spleen and an approximately 40% reduction in lymph nodes (Fig 1, *D-F*). These results indicate that although Treg cells function normally in uninfected perforin-deficient mice, FHL development is accompanied by a severe contraction in the Treg cell compartment.

To determine the basis for reduced Treg cell numbers during FHL, we phenotyped Treg cells from wild-type and $Prf1^{-/-}$ mice after LCMV infection. Treg cells from wild-type mice showed signs of activation during LCMV infection, with a transient increase in the percentage of Treg cells expressing CD69 (Fig 2, *A*), whereas CTLA4 (Fig 2, *B*) and CD103 (Fig 2, *C*)
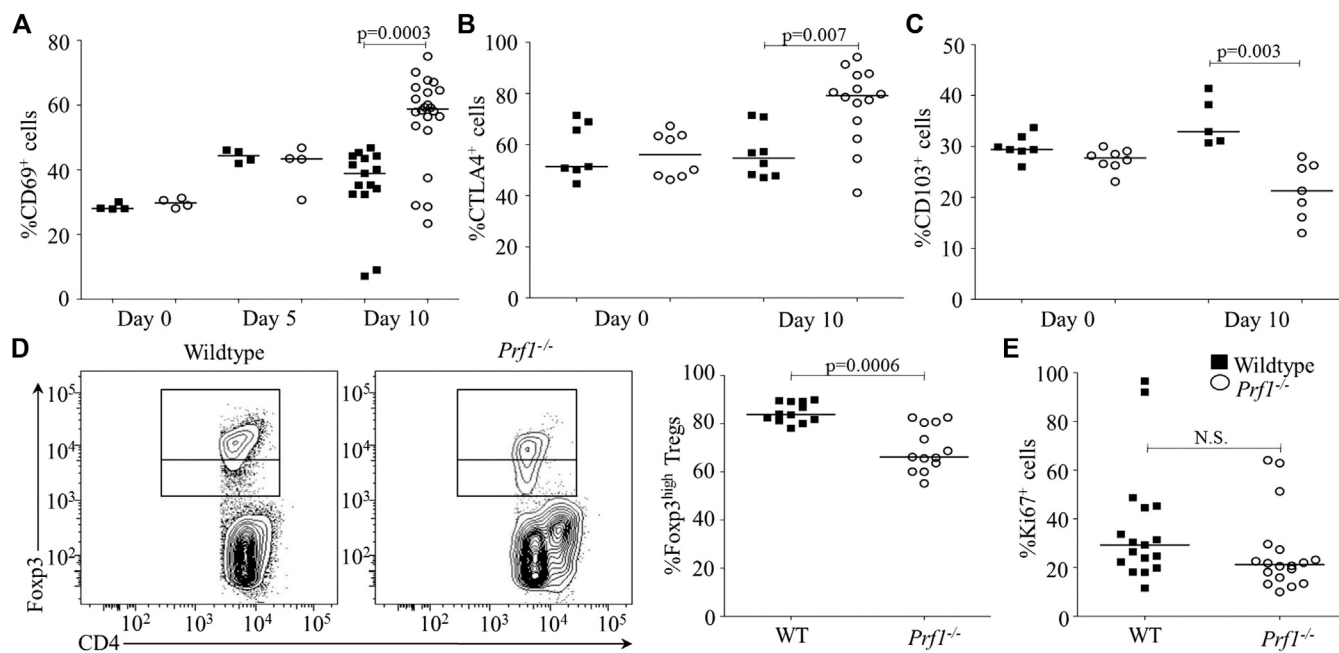
FIG 2. Differential activation of Treg cells during FHL inflammation. Wild-type and $Prf1^{-/-}$ mice were infected with LCMV-Armstrong and assessed for Treg cell activation profile in the lymph nodes. **A-C,** Expression of CD69 (Fig 2, *A*), CTLA4 (Fig 2, *B*), and CD103 (Fig 2, *C*) on Treg cells. **D,** Representative flow cytometric plot *(left)* and percentage *(right)* of Foxp3^{high} cells on total Foxp3^{+} Treg cells (day 10). **E,** Intracellular Ki67 expression in Treg cells (day 10). *WT,* Wild-type. Median and individual data points are shown. Results are pooled from 2 to 7 experiments.

expression remains stable. Treg cells from $Prf1^{-/-}$ mice infected with LCMV, by contrast, showed greater levels of activation, with a sustained upregulation of CD69 (Fig 2, *A*) and CTLA4 (Fig 2, *B*) that is consistent with the activation of Treg cells by inflammatory environments.[16] Paradoxically, expression of Foxp3 and CD103 was reduced on Treg cells from $Prf1^{-/-}$ mice in comparison with those from wild-type mice (Fig 2, *C* and *D*), and proliferation of Treg cells in the lymph nodes of $Prf1^{-/-}$ mice was dampened (Fig 2, *E*). Similar results were observed in the spleen (see Fig E2 in this article's Online Repository at www.jacionline.org). Because it has previously been demonstrated that IL-2 is required for optimal Foxp3 expression,[17] CD103 upregulation,[18] and Treg cell proliferation,[19] these results together suggest an impairment of the Treg–IL-2 homeostatic network. Together, these data demonstrate that an acquired peripheral Treg cell homeostasis defect develops in LCMV-infected $Prf1^{-/-}$ mice, but not wild-type mice, coincident with the hyperinflammatory state of HLH.

LCMV infection in perforin-deficient mice disrupts IL-2 consumption

To determine the proximal cause of defective Treg cell homeostasis in LCMV-infected perforin-deficient mice, we further investigated the IL-2 homeostatic network during murine HLH. Direct quantification of the low concentration of IL-2 present in mouse serum remains challenging. However, because the main source of IL-2 provision to Treg cells is CD4^{+} T cells,[20] IL-2 production could be measured. By using intracellular cytokine staining, IL-2 secretion was consistently lower in CD4^{+} T cells from infected $Prf1^{-/-}$ mice compared with wild-type mice (Fig 3, *A*). Moreover, because of the

hyperinflammatory status, total CD4^{+} T-cell counts were significantly decreased in both the spleens and lymph nodes of $Prf1^{-/-}$ compared with wild-type mice, exacerbating the defect in IL-2 production (Fig 3, *B*, and see Fig E3, *A*, in this article's Online Repository at www.jacionline.org). Absolute IL-2–producing CD4^{+} T-cell numbers decreased to an even greater extent (data not shown). By contrast, IL-2 production in CD8^{+} T cells was not modified by the loss of perforin (see Fig E4 in this article's Online Repository at www.jacionline.org). Indirect assessment of IL-2 consumption by Treg cells is possible by studying expression of CD25 (IL-2 receptor α) on the cell surface, which is closely correlated with IL-2 consumption levels because of a STAT5-dependent positive feedback loop mechanism that increases CD25 expression at the cell surface.[21] Analysis of mean fluorescence expression of CD25 on Treg cells in lymph nodes after infection showed a significant reduction of CD25 expression in $Prf1^{-/-}$ mice compared with that seen in wild-type mice, strongly supporting the hypothesis of a lack of access to IL-2 for the $Prf1^{-/-}$ Treg cells (Fig 3, *C*). By contrast, splenic Treg cells did not demonstrate reduced CD25 expression (see Fig E3, *B*); however, Mcl1 expression downstream of IL-2 signaling in Treg cells was reduced in LCMV-infected $Prf1^{-/-}$ Treg cells (Fig 3, *D*), which is consistent with the role of IL-2 in maintaining the prosurvival Mcl1,[19] providing a potential mechanistic explanation for the observed death of Treg cells.

Excessive CD8^{+} T-cell activation leads to reversal of IL-2 consumption hierarchy

IL-2 was discovered to be a potent T-cell growth factor,[22] with the immunoregulatory function of IL-2 generated by a consumption hierarchy whereby Treg cells express higher levels
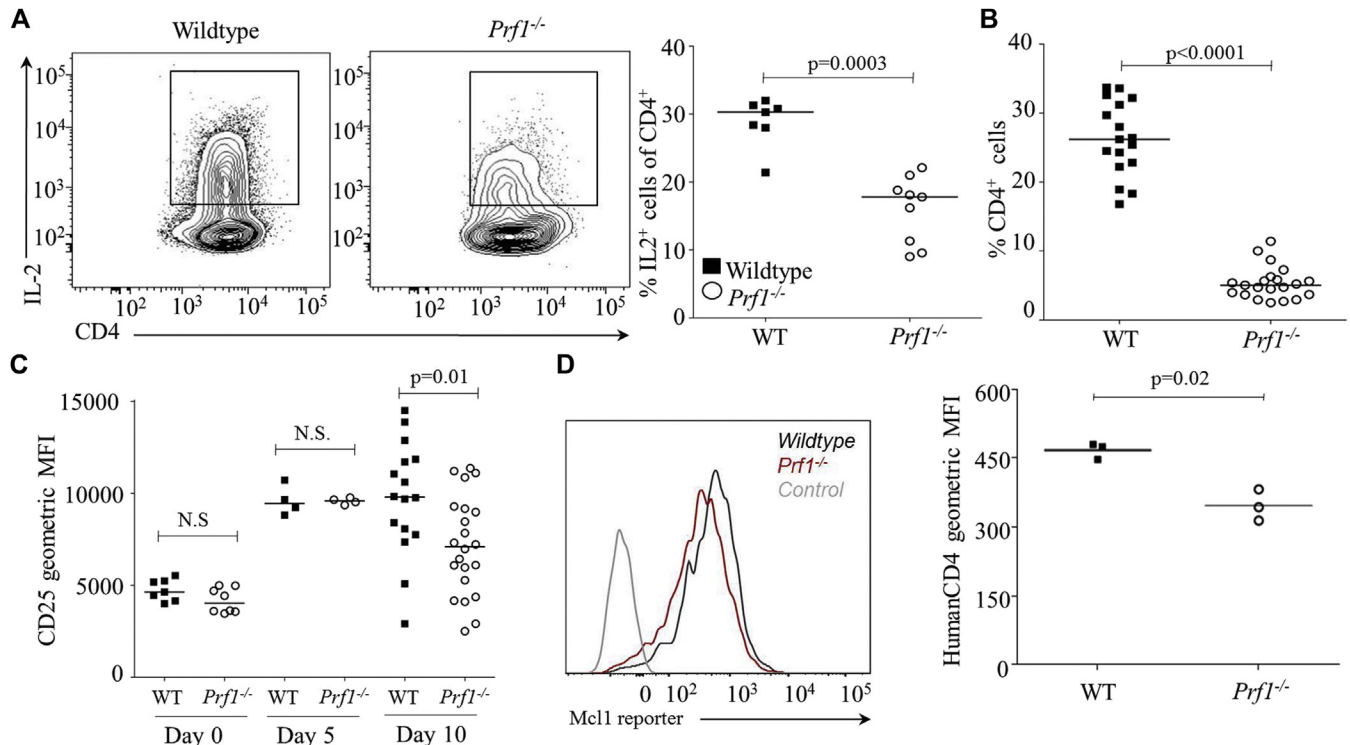
FIG 3. Limiting IL-2 availability in perforin-deficient mice during LCMV-triggered inflammation. Total CD4$^+$ T cells and IL-2 secretion were assessed in the lymph nodes of wild-type and $Prf1^{-/-}$ mice at day 10 after LCMV infection. **A,** IL-2 secretion by CD4$^+$ T cells, with representative flow cytometric plot *(left)* and graph *(right)*. **B,** Percentage of CD4$^+$ cells within total lymphocytes. **C,** CD25 mean fluorescence intensity *(MFI)* in the CD25$^+$ Treg cell population. *N.S.,* Not significant. **D,** Expression of huCD4 reporter for Mcl1 expression in splenic Foxp3$^+$ Treg cells from $CD127^{Cre}Mcl1^{wt/fl}Prf1^{wt/wt}$ and $CD127^{Cre}Mcl1^{wt/fl}Prf1^{-/-}$ mice (n = 3 mice per group). Representative histogram *(left)* and geometric mean fluorescence intensity (*MFI; right*) are shown. Median and individual data points are shown. Fig 3, *A,* Representative of 3 experiments. Fig 3, *A-C,* Results pooled from 3 to 7 experiments.

of CD25 than effector T cells. This hierarchy for consumption not only allows IL-2 to function as a rheostat for Treg cell numbers[19,20] but is also a proposed mechanism for Treg cell suppression of effector T cells.[23] We investigated whether this consumption hierarchy remained intact during the IL-2–deprived inflammatory environment of murine HLH. LCMV infection results in a highly activated CD8$^+$ T-cell profile. In a wild-type mouse the immune reaction peaks around days 7 to 8 after viral exposure, whereas infection is controlled by day 10 with clearance of all viral particles (data not shown). Indeed, we observed that the majority of the CD8$^+$ T cells shifted from a naive to an effector profile from day 5 to day 10 in LCMV-infected wild-type mice (Fig 4, *A* and *B,* and see Fig E5, *A* in this article's Online Repository at www.jacionline.org). In $Prf1^{-/-}$ mice the activation profile at day 5 remained similar to that of wild-type mice; however, the activation to an effector memory status was much more profound by day 10 (Fig 4, *A* and *B,* and see Fig E5, *A*), which is consistent with poorer viral clearance. This excessive CD8$^+$ T-cell activation in LCMV-infected $Prf1^{-/-}$ mice was also demonstrated by the increased expression of activation molecules, such as CD69 (Fig 4, *C,* and see Fig E5, *B*) and intracellular IFN-γ (Fig 4, *D*). More striking was the very high numbers of CD25-expressing CD8$^+$ T cells in $Prf1^{-/-}$ mice on day 10, which in wild-type mice shows only a low transient increase (Fig 4, *E,* and see Fig E5, *C*).

CD8$^+$ T cells from $Prf1^{-/-}$ mice also showed much greater CD25 expression on a per-cell basis. This 14-fold increase of CD25 expression on activated CD8$^+$ T cells from $Prf1^{-/-}$ mice, coupled with the approximately 2-fold decrease of CD25 on Treg cells, inverts the normal hierarchy for IL-2 affinity, with activated CD8$^+$ T cells from $Prf1^{-/-}$ but not wild-type mice having higher CD25 expression than Treg cells (Fig 4, *F* and *G,* and see Fig E5, *D*). This resulting competitive advantage for IL-2 capture resulted in greatly enhanced IL-2 signaling capacity of activated CD8$^+$ T cells in $Prf1^{-/-}$ mice, with a very high level of phospho-STAT5 activity in CD8$^+$ T cells from LCMV-infected $Prf1^{-/-}$ mice compared with those from wild-type infected mice (Fig 4, *H* and *I,* and see Fig E5, *E*). The increase in CD25 expression on CD8$^+$ T cells is likely driven by a combination of increased antigenic stimulation (higher LCMV titers) and the autocrine effects of increased IFN-γ because *in vitro* modeling demonstrated that increased CD25 expression in CD8$^+$ T cells after T-cell receptor stimulation is reduced in IFN-γ–deficient CD8$^+$ T cells but can be restored by the addition of exogenous IFN-γ (Fig 5).

A high sCD25 level reflecting T-cell activation in the serum is one of the diagnostic criteria in patients with FHL.[1,2] This prompted us to measure sCD25 levels in our model. Importantly, we observed extremely high sCD25 levels in $Prf1^{-/-}$ mice sera compared with wild-type mice on day 10 after infection (Fig 6, *A*). This not only recapitulates a key component of FHL, but
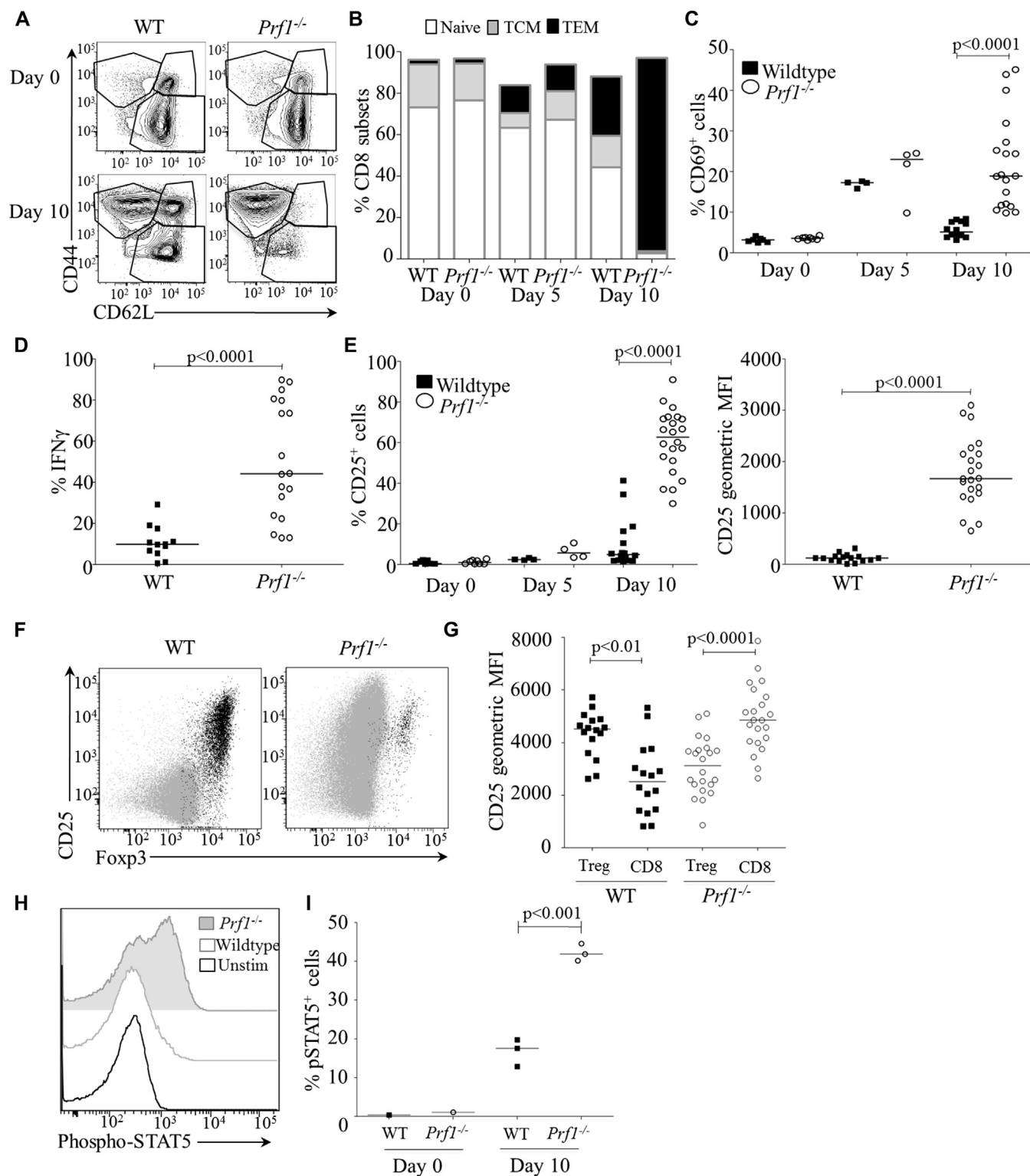
FIG 4. Excessive CD8^{+} T-cell activation inverts the IL-2 consumption hierarchy in perforin-deficient mice. Wild-type and $Prf1^{-/-}$ mice were infected with LCMV-Armstrong and assessed at days 0, 5, and 10 for CD8^{+} T-cell activation in the lymph nodes. **A,** CD8^{+} T-cell subpopulations were characterized as CD8^{+}CD62L^{+}CD44^{−} naive cells, CD8^{+}CD62L^{+}CD44^{+} central memory T cells *(TCM)*, and CD8^{+}CD62L^{−}CD44^{+} effector memory T cells *(TEM)* by means of flow cytometry. **B,** Percentage of CD8^{+} naive, TCM, and TEM cells. **C-E,** Percentage of CD8^{+} T cells expressing CD69 (Fig 4, *C*), intracellular IFN-γ (on day 10; Fig 4, *D*), and CD25 *(left)* and CD25 geometric mean fluorescence intensity on total CD8^{+} T cells at day 10 *(right;* Fig 4, *E*). **F** and **G,** Representative flow cytometry profiles of CD25 expression on CD8^{+} T cells *(gray)* and Treg cells *(black)* in wild-type and $Prf1^{-/-}$ mice on day 10 (Fig 4, *F*) and geometric mean fluorescence
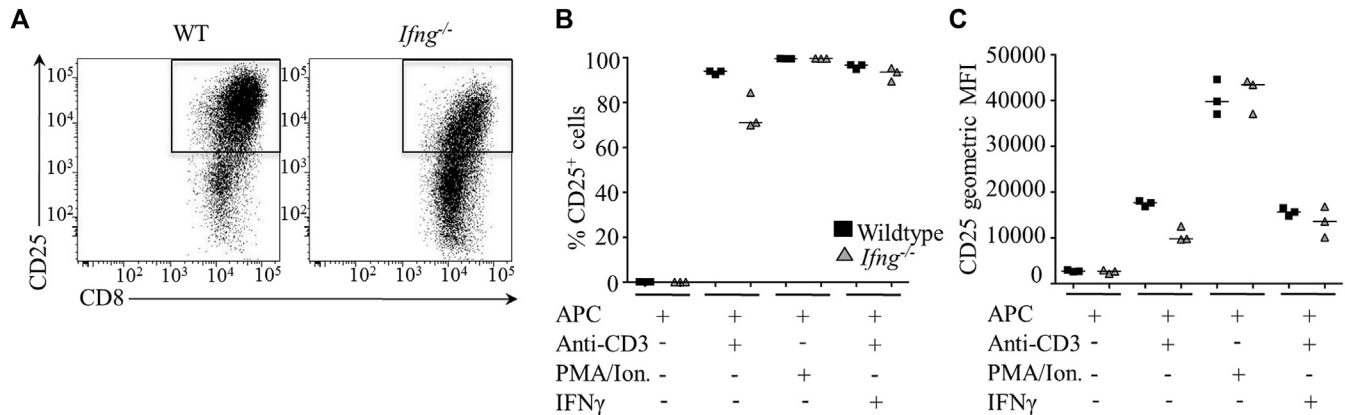
FIG 5. Synergistic effects of anti-CD3 stimulation and IFN-γ on CD25 expression by CD8^{+} T cells. Wild-type and $Ifng^{-/-}$ CD8^{+} T cells were stimulated *in vitro* and analyzed for CD25 expression by using flow cytometry. **A,** Representative flow cytometry profiles of CD25 expression on CD8^{+} T cells from wild-type and $Ifng^{-/-}$ mice. **B** and **C,** Percentage of CD8^{+} T cells expressing CD25 (Fig 5, *B*) and geometric mean fluorescence intensity *(MFI)* on CD25^{+}CD8^{+} T cells (Fig 5, *C*). *APC,* Antigen-presenting cells; *PMA/Ion.,* phorbol 12-myristate 13-acetate/ionomycin. Median and individual data points are shown. Results are representative of 3 experiments.

because sCD25 might have the capacity to compete with CD25 for IL-2 binding,[24] it adds an additional mechanism by which bioavailable IL-2 becomes limiting in $Prf1^{-/-}$ mice after LCMV infection. Because of the greatly increased level of CD25 expression on CD8^{+} T cells (Fig 4, *F*), we investigated CD8^{+} T cells as a source for sCD25. Within infected mice, there was a significant correlation between sCD25 levels and CD25 expression on the surface of CD8^{+} T cells (Fig 6, *B,* and see Fig E6 in this article's Online Repository at www.jacionline. org), and *in vitro* activated CD8^{+} T cells shed sCD25 into the supernatant (Fig 6, *C*). Overall, these data show that uncontrolled activation of CD8^{+} T cells during LCMV-triggered inflammation in $Prf1^{-/-}$ mice contributes to IL-2 deficiency through competitive IL-2 consumption and sCD25 shedding.

Diversion of the IL-2 negative feedback regulatory network into an inflammatory feed-forward network

The homeostatic IL-2 regulatory network allows *in vivo* expansion of Treg cells through supplementation of IL-2 to supraphysiologic levels with IL-2/anti–IL-2 antibody complexes.[25] Therefore we sought to determine whether we could prevent lethal HLH in $Prf1^{-/-}$ mice by treating with IL-2 complexes during LCMV infection. Surprisingly, initial experiments resulted in more rapid death of LCMV-infected $Prf1^{-/-}$ mice, with most IL-2 complex–treated mice dying before day 10 (data not shown). Analysis of LCMV-infected $Prf1^{-/-}$ mice with and without IL-2 complex treatment demonstrated that the additional IL-2 provision was able to restore the high level of CD25 expression on the Treg cell surface (Fig 7, *A*), driving proliferation (Fig 7, *B*) and increasing the size of the Treg cell compartment in some mice (Fig 7, *C*). However, this significant improvement toward

immunosuppression was overridden by the counterproductive effect on CD8^{+} T cells, which (as CD25^{high} cells) also received increased IL-2 signal, as reflected by a further increase in CD25 levels (Fig 7, *D*) and expansion (Fig 7, *E*). Critical for disease progression, IL-2 complex treatment of $Prf1^{-/-}$ mice also increased IFN-γ production (Fig 7, *F*), the distal pathogenic event in HLH. Similar results were observed in the spleen (see Fig E7 in this article's Online Repository at www.jacionline.org). In all, these data demonstrate that the excessive activation of $Prf1^{-/-}$ CD8^{+} T cells during LCMV infection results in both a reduction of bioavailable IL-2 for Treg cells and also a diversion of IL-2 consumption from the anti-inflammatory Treg cell circuit to a proinflammatory effector CD8^{+} T-cell circuit. These results suggest that altered IL-2 homeostasis contributes to the proximal defects driving fatal inflammation during HLH and FHL.

Patients with FHL/MAS experience low Treg cell numbers during inflammatory flares

To provide proof-of-principle translation to the clinical setting, we assessed patients with newly diagnosed FHL or MAS for Treg cell numbers as part of clinical diagnostics (see Table E1 in this article's Online Repository at www.jacionline.org). Seven patients with active FHL or MAS were assessed for Treg cell numbers. Because of the rapid progression of disease, 4 patients had already received treatment before blood sample analysis. Of the untreated patients, all exhibited Treg cell frequencies in the peripheral blood of less than the diagnostic standard range (Fig 8). However, of the 4 patients who had already started corticosteroids, cyclosporine treatment, or both, 3 had Treg cell frequencies within the standard range, and the 1 patient with low Treg cell numbers after treatment died (Fig 8). Together, these data demonstrate that the Treg cell count decrease observed

◄──────

intensity for CD25 expression on Foxp3^{+} Treg cells and CD25^{+}CD8^{+} T cells, as assessed by using a paired *t* test. **H** and **I,** Representative flow cytometry histogram of phospho-STAT5 gated on CD8^{+} T cells in unstimulated control *(black line),* wild-type *(gray line),* and $Prf1^{-/-}$ mice *(gray line with filled area)* 10 days after LCMV infection (Fig 4, *H*) and percentage of positive phospho-STAT5 within CD8^{+} T cells (Fig 4, *I*). *MFI,* Mean fluorescence intensity; *WT,* wild-type. Fig 4, *A* and *F,* Representative of 7 experiments. Fig 4, *H* and *I,* Representative of 1 to 2 experiments. Fig 4, *B-E* and *G,* Results pooled from 2 to 7 experiments.
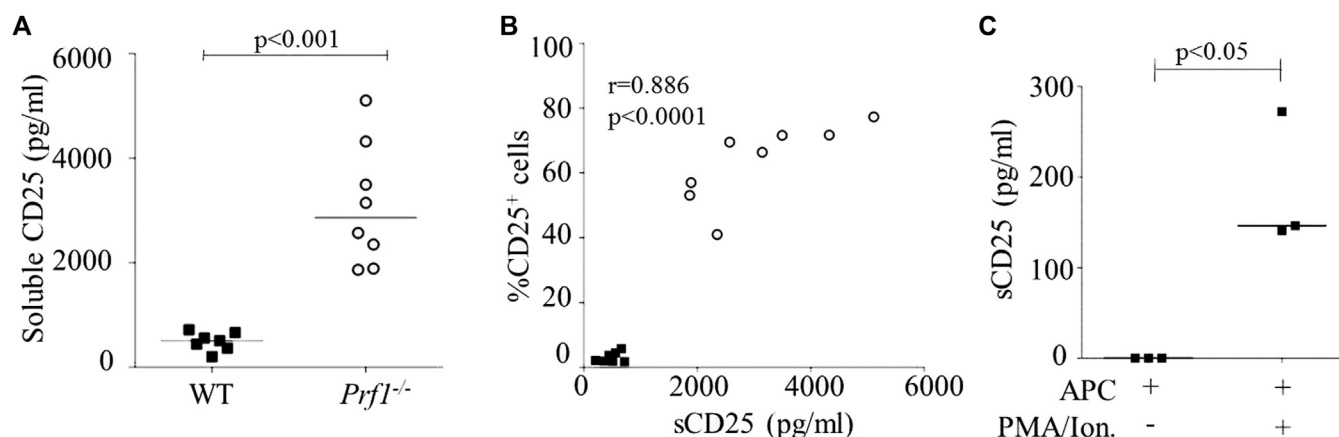
FIG 6. Increased secretion of sCD25 by activated CD8^{+} T cells during FHL. **A,** sCD25 in serum from wild-type *(WT)* and *Prf1*^{−/−} mice at day 10 after LCMV infection. **B,** Correlation between CD25-expressing CD8^{+} T cells in the lymph nodes with respective sCD25 concentrations in serum (day 10). **C,** Supernatant sCD25 measurement from *in vitro*–stimulated CD8^{+} T cells. *APC,* Antigen-presenting cells; *PMA/Ion.,* phorbol 12-myristate 13-acetate/ionomycin. Median and individual data points are shown. Data are pooled from 2 experiments.
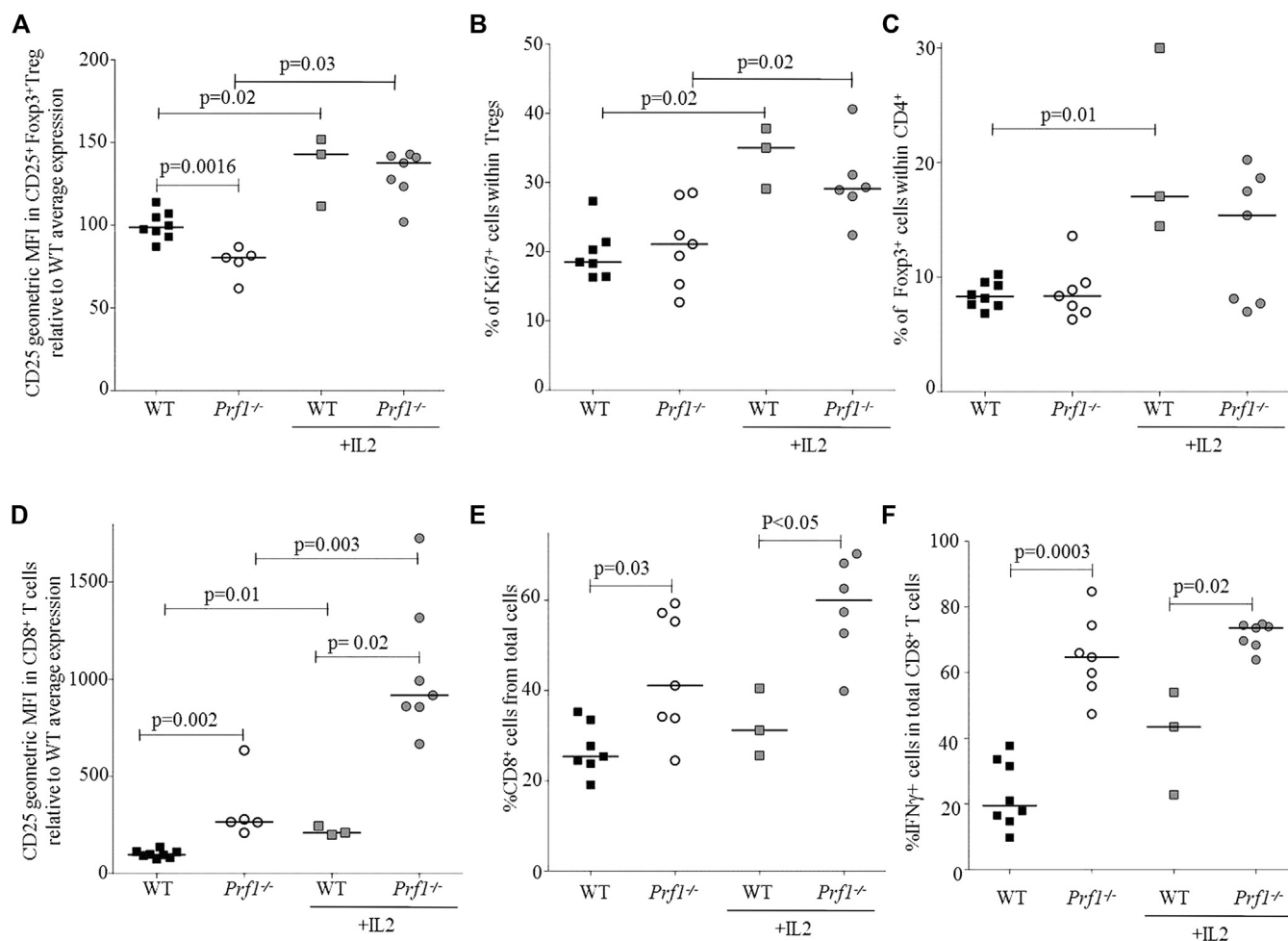

FIG 7. IL-2 elicits a feed-forward inflammatory loop during LCMV-triggered disease. Wild-type *(WT)* and *Prf1*^{−/−} mice, with or without IL-2 complex treatment, were infected with LCMV-Armstrong. **A-C,** Lymph node Treg cell counts were assessed (day 8) for CD25 geometric mean fluorescence intensity within CD25^{+} cells (Fig 7, *A*), Ki67 expression (Fig 7, *B*), and percentage within CD4^{+} T cells (Fig 7, *C*). **D-F,** CD8^{+} T cells were assessed for CD25 geometric mean fluorescence intensity (Fig 7, *D*), percentage within lymphocytes (Fig 7, *E*), and IFN-γ expression (Fig 7, *F*). *MFI,* Mean fluorescence intensity. Median and individual data points are shown and pooled from 3 experiments.
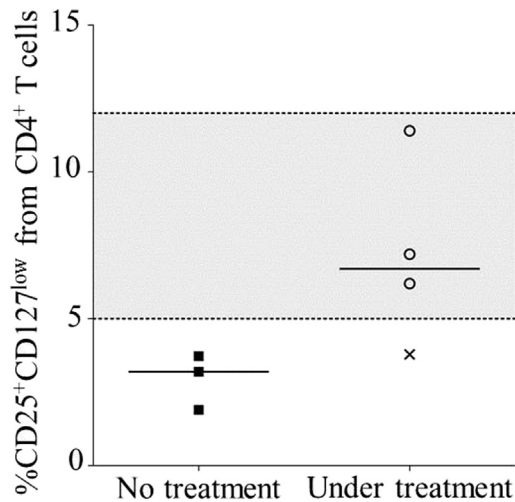
FIG 8. Low Treg cell numbers in patients with untreated FHL/MAS. Peripheral blood from patients with an acute FHL/MAS episode were assessed for the percentage of Treg cells (CD4$^+$CD25$^+$CD127^{low}). Patients were assessed before or after treatment. Fatality is indicated with an X. Median and individual data points are shown. The healthy standard range is represented in the *gray shaded area.*

during murine FHL is paralleled in FHL/MAS in clinical patients and suggest that immunosuppression restores Treg cell frequency. We also note that the first patient with Treg cell–deficient IPEX syndrome to undergo bone marrow transplantation had low donor chimerism and later died of HLH.[26] Together, these data indicate that transient Treg cell deficiency warrants further investigation as a potential contributor to the proinflammatory environment during clinical FHL/MAS. Such an effect might be driven by the compounding effects of altered CD25 expression and reduced IL-2 production and sCD25 levels, as we observe here in mice, or in the patient context it might be primarily driven by the high sCD25 level, which is already known to define FHL/MAS.

DISCUSSION

In this report we describe the fate of Treg cells under the debilitating condition of LCMV-induced FHL. We demonstrated that after excessive activation of CD8$^+$ T cells, IL-2 production is reduced and the consumption hierarchy is reversed, leading to preferential consumption by inflammatory CD8$^+$ T cells to the detriment of anti-inflammatory Treg cells.

Under physiologic conditions, Treg cells are important actors in peripheral immune tolerance, creating a buffer against spontaneous immune activation. Nevertheless, immune activation is necessary during infection, and thus the Treg cell immunosuppression needs to be robust while also being surmountable. In a recent report Srivasatva et al[27] showed that wild-type mice have a transient decrease in Treg cell numbers during LCMV infection, an effect secondary to type I interferon signaling and one that allows a proper immune reaction against the virus. Consistent with this, Treg cells from wild-type mice showed the same kinetic profile in our study. Therefore a transient dip in Treg cell numbers is a normal and even productive component of a strong inflammatory response against viral stimuli. However, our data indicate that in *Prf1*$^{-/-}$ mice the level of CD8$^+$ T-cell immune activation crosses a critical threshold, at which point the CD8$^+$

T cells become capable of diverting the normally anti-inflammatory IL-2 feedback loop into a proinflammatory circuit, driving the precipitous decrease in Treg cell numbers and feed-forward inflammation. Several synergistic events appear to participate in this process, with IL-2 production by CD4$^+$ T cells being suppressed[28] (an effect that might be mediated directly by IFN-γ[29]) and release of sCD25 by CD8$^+$ T cells and reversal of the CD25 expression hierarchy allowing preferential consumption of IL-2 by CD8$^+$ T cells at the expense of Treg cells. Critically, this inverted hierarchy meant that IL-2 supplementation, which is normally protective in patients with Treg cell deficiencies, drove excessive CD8$^+$ T-cell activation and led to the premature death of *Prf1*$^{-/-}$ mice.

A critical component of the IL-2 feedback loops is the relation between IL-2 availability and CD25 expression. In the homeostatic state CD25 expression is essentially absent on effector T cells, whereas it is a defining characteristic of Treg cells, creating the consumption hierarchy.[30,31] However, it is noteworthy that inflammatory stimuli can upregulate CD25 on CD8$^+$ T cells independent of the addition of IL-2,[32] as shown also by our *in vitro* experiment. Moreover, on the Treg cell side, reduced IL-2 uptake will decrease Foxp3 expression, which in turn will not sustain CD25^{high} expression at the cell surface.[21] Thus the normal transient events that occur during the early response after viral infection in wild-type mice serve to reduce the disparity in IL-2 consumptive capacity, creating an immunologic context in which strongly reactive effector CD8$^+$ T cells can expand in a controlled manner. Once antigen stimulation is removed, however, Treg cells regain disproportionately high CD25 expression and thereby limit IL-2 availability for other effector cells driving immune contraction.[30,31] In the context of HLH, however, the transient tempering of the Treg cell IL-2 consumptive advantage is pushed even further by the defective clearance of the viral trigger to allow highly activated CD8$^+$ T cells to literally consume all available IL-2 to the detriment of Treg cells. This rewiring of the IL-2 network results in a destructive immune situation, which is acquired parallel to the primary Treg cell deficiency of IPEX syndrome. Although the primary genetic cause of the IL-2 network imbalance in patients with FHL is a genetic defect in the perforin pathway (increasing the chronicity of the CD8$^+$ T response), it is notable that this rewiring could be driven by any immunologic event in which CD8$^+$ T-cell activation exceeds a certain threshold, such as occurs during *Toxoplasma gondii* infection in mice,[29] or the numerous nongenetic precipitating events in patients with HLH. Regardless of the initial event, however, the acquired Treg cell depletion will contribute to the severity of the inflammatory environment and in particular to the extension of infection-associated inflammation into persistent inflammation.

Overall, this study raises the possibility that HLH belongs in the expanding set of Treg cell homeostasis disorders by identifying the important role of the IL-2 network dysregulation in patients with HLH. Furthermore, the underlying biology of this dysregulation, with a reversal of the normal consumption hierarchy, makes the disease refractory to IL-2 supplementation. Indeed, 3 different clinical reports have shown positive clinical outcomes in patients with HLH treated with anti-CD25 mAbs,[33-35] whereas the efficacious cyclosporine treatment directly suppresses IL-2 expression.[36] Although it is counterintuitive that a disease of Treg cell homeostatic dysregulation would positively respond to treatments that suppress IL-2 availability,

this result is reconciled by the consideration that IL-2 is performing the inverse (proinflammatory) function in patients with HLH. These results suggest that the most efficacious treatment route for HLH would be one in which CD8$^+$ T-cell activation is inhibited while allowing Treg cell homeostasis to recover, restoring the IL-2 homeostatic network to its anti-inflammatory function, although further investigation of the patient context would be required before any change to current treatment strategies could be tested.

Key messages

- **Treg cell numbers are severely decreased during murine FHL.**

- **Excessively activated CD8$^+$ T cells during FHL outcompete Treg cells for IL-2.**

- **Untreated patients with FHL/HLH experience Treg cell reduction.**

REFERENCES

1. Janka GE, Lehmberg K. Hemophagocytic lymphohistiocytosis: pathogenesis and treatment. Hematology Am Soc Hematol Educ Program 2013;2013: 605-11.
2. Usmani GN, Woda BA, Newburger PE. Advances in understanding the pathogenesis of HLH. Br J Haematol 2013;161:609-22.
3. Jordan MB, Allen CE, Weitzman S, Filipovich AH, McClain KL. How I treat hemophagocytic lymphohistiocytosis. Blood 2011;118:4041-52.
4. Jordan MB, Hildeman D, Kappler J, Marrack P. An animal model of hemophagocytic lymphohistiocytosis (HLH): CD8+ T cells and interferon gamma are essential for the disorder. Blood 2004;104:735-43.
5. Sepulveda FE, Debeurme F, Menasche G, Kurowska M, Cote M, Pachlopnik Schmid J, et al. Distinct severity of HLH in both human and murine mutants with complete loss of cytotoxic effector PRF1, RAB27A, and STX11. Blood 2013;121:595-603.
6. Terrell CE, Jordan MB. Perforin deficiency impairs a critical immunoregulatory loop involving murine CD8(+) T cells and dendritic cells. Blood 2013;121: 5184-91.
7. Malloy CA, Polinski C, Alkan S, Manera R, Challapalli M. Hemophagocytic lymphohistiocytosis presenting with nonimmune hydrops fetalis. J Perinatol 2004;24:458-60.
8. Nitta A, Suzumura H, Watabe Y, Okuya M, Nakajima D, Kurosawa H, et al. Fetal hemophagocytic lymphohistiocytosis in a premature infant. J Pediatr 2007;151:98.
9. Janka GE, Lehmberg K. Hemophagocytic syndromes—an update. Blood Rev 2014;28:135-42.
10. Humblet-Baron S, Sather B, Anover S, Becker-Herman S, Kasprowicz DJ, Khim S, et al. Wiskott-Aldrich syndrome protein is required for regulatory T cell homeostasis. J Clin Invest 2007;117:407-18.
11. Miyara M, Gorochov G, Ehrenstein M, Musset L, Sakaguchi S, Amoura Z. Human FoxP3+ regulatory T cells in systemic autoimmune diseases. Autoimmun Rev 2011;10:744-55.
12. Schlenner SM, Madan V, Busch K, Tietz A, Laufle C, Costa C, et al. Fate mapping reveals separate origins of T cells and myeloid lineages in the thymus. Immunity 2010;32:426-36.
13. Vikstrom I, Carotta S, Luthje K, Peperzak V, Jost PJ, Glaser S, et al. Mcl-1 is essential for germinal center formation and B cell memory. Science 2010;330: 1095-9.
14. Utzschneider DT, Legat A, Fuertes Marraco SA, Carrie L, Luescher I, Speiser DE, et al. T cells maintain an exhausted phenotype after antigen withdrawal and population reexpansion. Nat Immunol 2013;14:603-10.
15. Butz EA, Bevan MJ. Massive expansion of antigen-specific CD8+ T cells during an acute virus infection. Immunity 1998;8:167-75.
16. Tian L, Humblet-Baron S, Liston A. Immune tolerance: are regulatory T cell subsets needed to explain suppression of autoimmunity? Bioessays 2012;34: 569-75.
17. Fontenot JD, Rasmussen JP, Gavin MA, Rudensky AY. A function for interleukin 2 in Foxp3-expressing regulatory T cells. Nat Immunol 2005;6:1142-51.
18. Sharma R, Sung SS, Abaya CE, Ju AC, Fu SM, Ju ST. IL-2 regulates CD103 expression on CD4+ T cells in Scurfy mice that display both CD103-dependent and independent inflammation. J Immunol 2009;183:1065-73.
19. Pierson W, Cauwe B, Policheni A, Schlenner SM, Franckaert D, Berges J, et al. Antiapoptotic Mcl-1 is critical for the survival and niche-filling capacity of Foxp3(+) regulatory T cells. Nat Immunol 2013;14:959-65.
20. Amado IF, Berges J, Luther RJ, Mailhe MP, Garcia S, Bandeira A, et al. IL-2 coordinates IL-2-producing and regulatory T cell interplay. J Exp Med 2013; 210:2707-20.
21. Malek TR, Castro I. Interleukin-2 receptor signaling: at the interface between tolerance and immunity. Immunity 2010;33:153-65.
22. Smith KA. Interleukin-2. Curr Opin Immunol 1992;4:271-6.
23. Vignali DA, Collison LW, Workman CJ. How regulatory T cells work. Nat Rev Immunol 2008;8:523-32.
24. Russell SE, Moore AC, Fallon PG, Walsh PT. Soluble IL-2Ralpha (sCD25) exacerbates autoimmunity and enhances the development of Th17 responses in mice. PLoS One 2012;7:e47748.
25. Boyman O, Kovar M, Rubinstein MP, Surh CD, Sprent J. Selective stimulation of T cell subsets with antibody-cytokine immune complexes. Science 2006;311: 1924-7.
26. Baud O, Goulet O, Canioni D, Le Deist F, Radford I, Rieu D, et al. Treatment of the immune dysregulation, polyendocrinopathy, enteropathy, X-linked syndrome (IPEX) by allogeneic bone marrow transplantation. N Engl J Med 2001;344: 1758-62.
27. Srivastava S, Koch MA, Pepper M, Campbell DJ. Type I interferons directly inhibit regulatory T cells to allow optimal antiviral T cell responses during acute LCMV infection. J Exp Med 2014;211:961-74.
28. Benson A, Murray S, Divakar P, Burnaevskiy N, Pifer R, Forman J, et al. Microbial infection-induced expansion of effector T cells overcomes the suppressive effects of regulatory T cells via an IL-2 deprivation mechanism. J Immunol 2012;188: 800-10.
29. Oldenhove G, Bouladoux N, Wohlfert EA, Hall JA, Chou D, Dos Santos L, et al. Decrease of Foxp3+ Treg cell number and acquisition of effector cell phenotype during lethal infection. Immunity 2009;31:772-86.
30. Boyman O, Sprent J. The role of interleukin-2 during homeostasis and activation of the immune system. Nat Rev Immunol 2006;12:180-90.
31. Kastenmuller W, Gasteiger G, Subramanian N, Sparwasser T, Busch DH, Belkaid Y, et al. Regulatory T cells selectively control CD8+ T cell effector pool size via IL-2 restriction. J Immunol 2011;187:3186-97.
32. Pipkin ME, Sacks JA, Cruz-Guilloty F, Lichtenheld MG, Bevan MJ, Rao A. Interleukin-2 and inflammation induce distinct transcriptional programs that promote the differentiation of effector cytolytic T cells. Immunity 2010;32:79-90.
33. Lackner H, Urban C, Sovinz P, Benesch M, Moser A, Schwinger W. Hemophagocytic lymphohistiocytosis as severe adverse event of antineoplastic treatment in children. Haematologica 2008;93:291-4.
34. Olin RL, Nichols KE, Naghashpour M, Wasik M, Shelly B, Stadtmauer EA, et al. Successful use of the anti-CD25 antibody daclizumab in an adult patient with hemophagocytic lymphohistiocytosis. Am J Hematol 2008;83:747-9.
35. Tomaske M, Amon O, Bosk A, Handgretinger R, Schneider EM, Niethammer D. Alpha-CD25 antibody treatment in a child with hemophagocytic lymphohistiocytosis. Med Pediatr Oncol 2002;38:141-2.
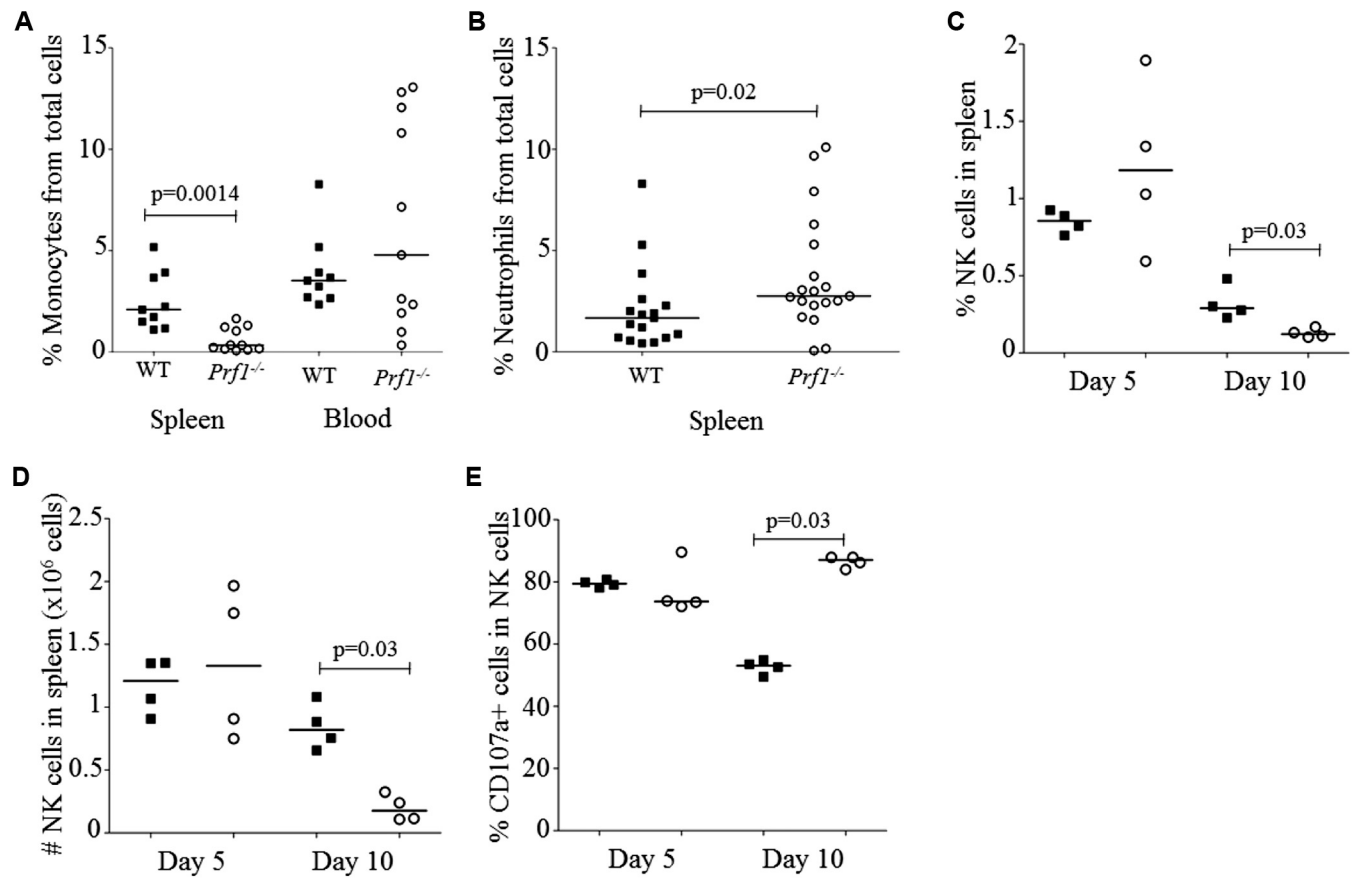36. Macian F. NFAT proteins: key regulators of T-cell development and function. Nat Rev Immunol 2005;5:472-84.

FIG E1. Altered leukocyte compartment during FHL. Leukocyte subsets were analyzed in *Prf1*$^{-/-}$ mice at day 10 after LCMV infection. **A,** Percentage of monocytes in spleen and blood. **B,** Percentage of neutrophils in spleen. **C,** Percentage of natural killer *(NK)* cells in the spleen defined as NK1-1$^+$NKp46$^+$ cells. **D,** Absolute NK cells in the spleen. **E,** Upregulation of CD107a in NK cells in the spleen. Median and individual data points are shown. Fig E1, *A* and *B*, Results pooled from 7 experiments. Fig E1, *C-E*, Single experiment. *WT*, Wild-type.
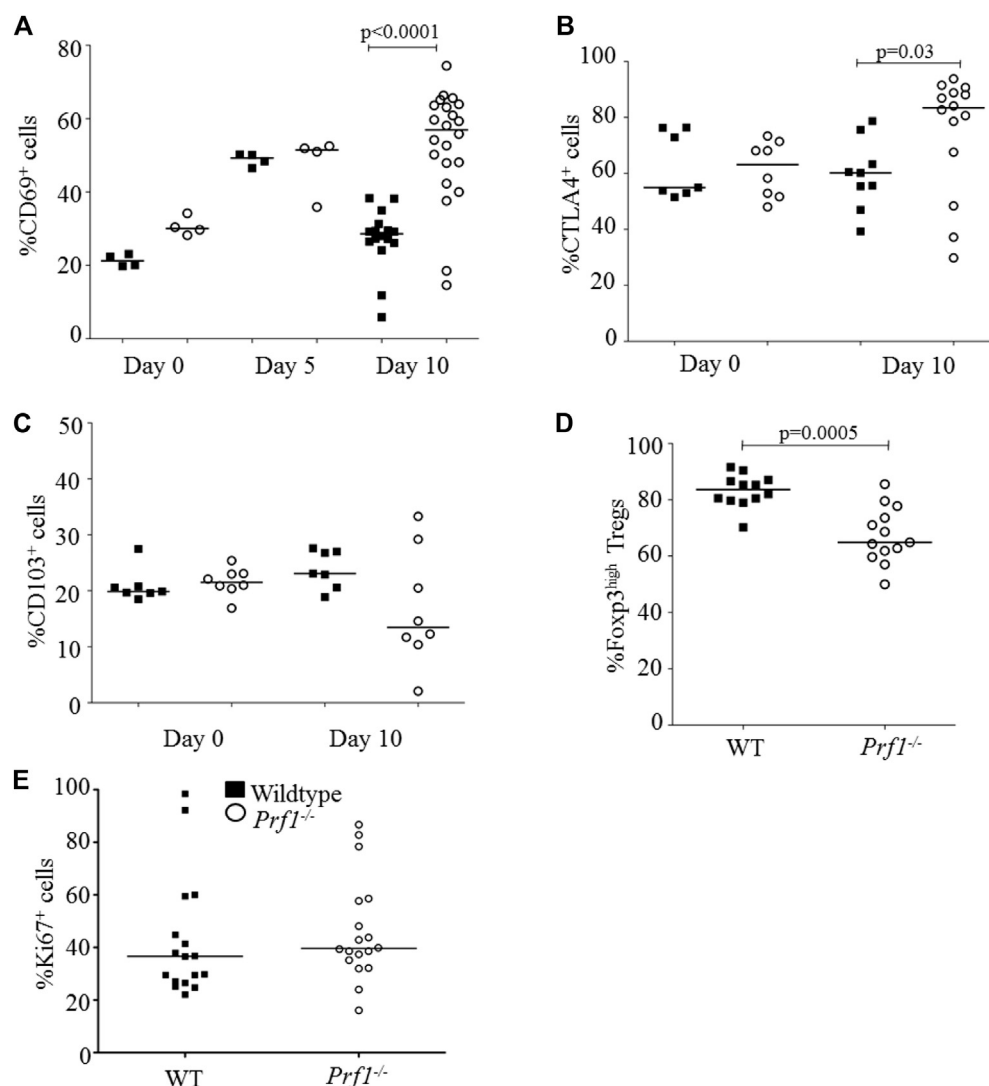
FIG E2. Differential activation of Treg cells during FHL inflammation. Wild-type and $Prf1^{-/-}$ mice were infected with LCMV-Armstrong and assessed at days 0, 5, and 10 for Treg cell activation profiles in the spleen. **A-C,** Expression of CD69 (Fig E2, *A*), CTLA4 (Fig E2, *B*), and CD103 (Fig E2, *C*) on Treg cells from wild-type and $Prf1^{-/-}$ mice. **D,** Percentage of Foxp3^{high} cells on total Foxp3$^+$ Treg cells in wild-type and $Prf1^{-/-}$ mice at day 10 after LCMV infection. **E,** Intracellular Ki67 expression in Treg cells in spleen on day 10 after LCMV infection. *WT*, Wild-type. Median and individual data points are shown. Results are pooled from 2 to 7 experiments.
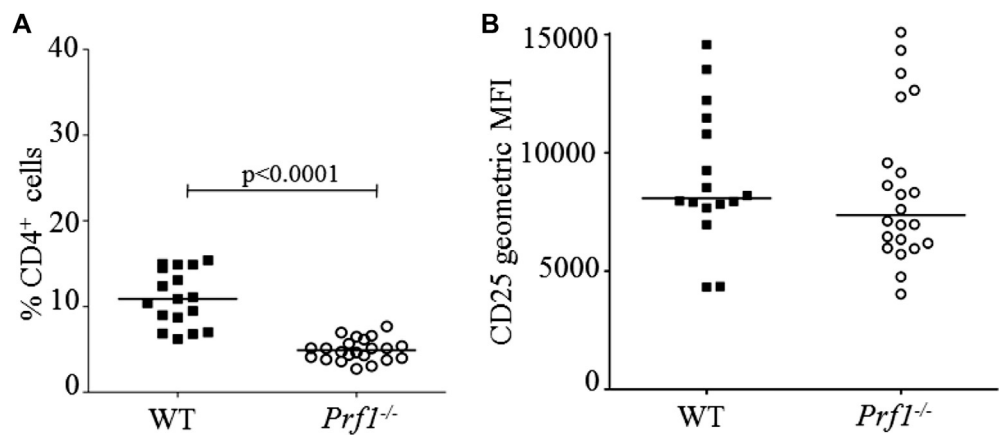
FIG E3. Limiting IL-2 availability in perforin-deficient mice during LCMV-triggered inflammation. Total CD4$^+$ T cells and IL-2 secretion were assessed in wild-type and $Prf1^{-/-}$ mice at day 10 after LCMV infection. **A,** Percentage of CD4$^+$ cells of total lymphocytes in the spleens of wild-type and $Prf1^{-/-}$ mice. **B,** CD25 expression determined by using geometric mean fluorescence intensity *(MFI)* in the splenic CD25$^+$ Treg cell population. *WT,* Wild-type. Median and individual data points are shown. Results are pooled from 3 to 7 experiments.
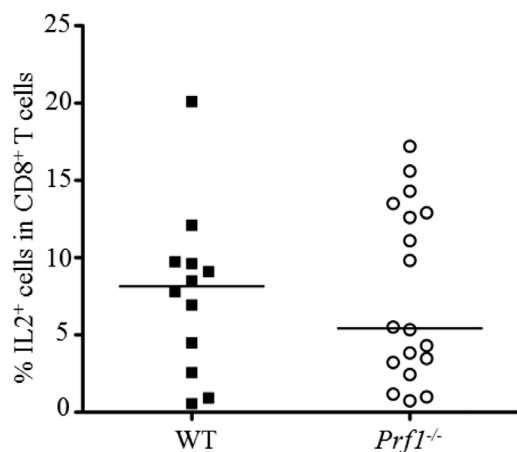
FIG E4. IL-2 production by CD8$^+$ T cells is unchanged by perforin deficiency. Total CD8$^+$ T cells and IL-2 secretion were assessed in wild-type *(WT)* and *Prf1*$^{-/-}$ mice at day 10 after LCMV infection by using flow cytometry. Percentage of IL-2 secreted by CD8$^+$ cells in the lymph nodes of wild-type and *Prf1*$^{-/-}$ mice. Results are pooled from 6 experiments.
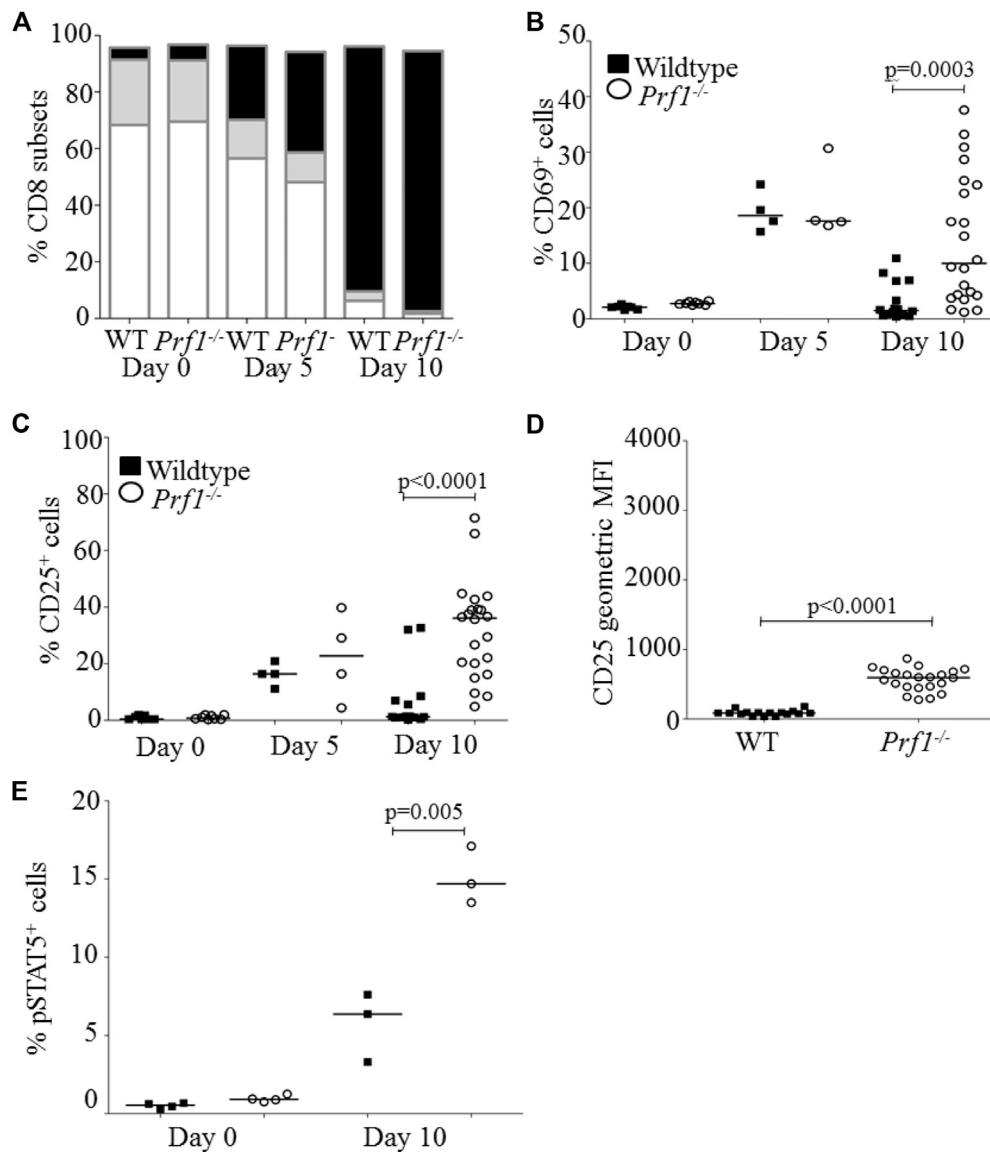
FIG E5. Excessive CD8$^+$ T-cell activation inverts the IL-2 consumption hierarchy in perforin-deficient mice. Wild-type and *Prf1*$^{-/-}$ mice were infected with LCMV-Armstrong and assessed at days 0, 5, and 10 for CD8$^+$ T-cell activation in the spleen. **A,** CD8$^+$ T-cell subpopulations were characterized as CD8$^+$CD62L$^+$CD44$^-$ naive cells, CD8$^+$CD62L$^+$CD44$^+$ central memory T cells *(TCM)*, and CD8$^+$CD62L$^-$CD44$^-$ effector memory T cells *(TEM)* by using flow cytometry. The percentage of CD8$^+$ naive, TCM, and TEM cells in wild-type mice and *Prf1*$^{-/-}$ mice after LCMV infection is shown. **B-D,** Percentage of CD8$^+$ T cells expressing CD69 (Fig E5, *B*), CD25 (Fig E5, *C*), and CD25 geometric mean fluorescence intensity (*MFI*; Fig E5, *D*) on total CD8$^+$ T cells at day 10 after LCMV infection. **E,** Percentage of positive phospho-STAT5 within the CD8$^+$ T-cell population at days 0 and 10 after LCMV infection. Fig E5, *A-D*, Results pooled from 2 to 7 experiments. Fig E5, *E*, Representative of 1 to 2 experiments.
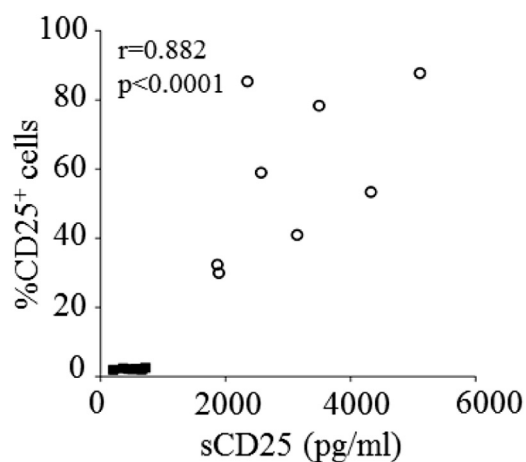
FIG E6. Increased secretion of sCD25 by activated CD8^{+} T cells during FHL. Correlation between the percentage of splenic CD25-expressing CD8^{+} T cells from wild-type and *Prf1*^{−/−} mice with their respective sCD25 concentrations in serum is shown. The Spearman *r* value is 0.882. Median and individual data points are shown. Data are pooled from 2 experiments.
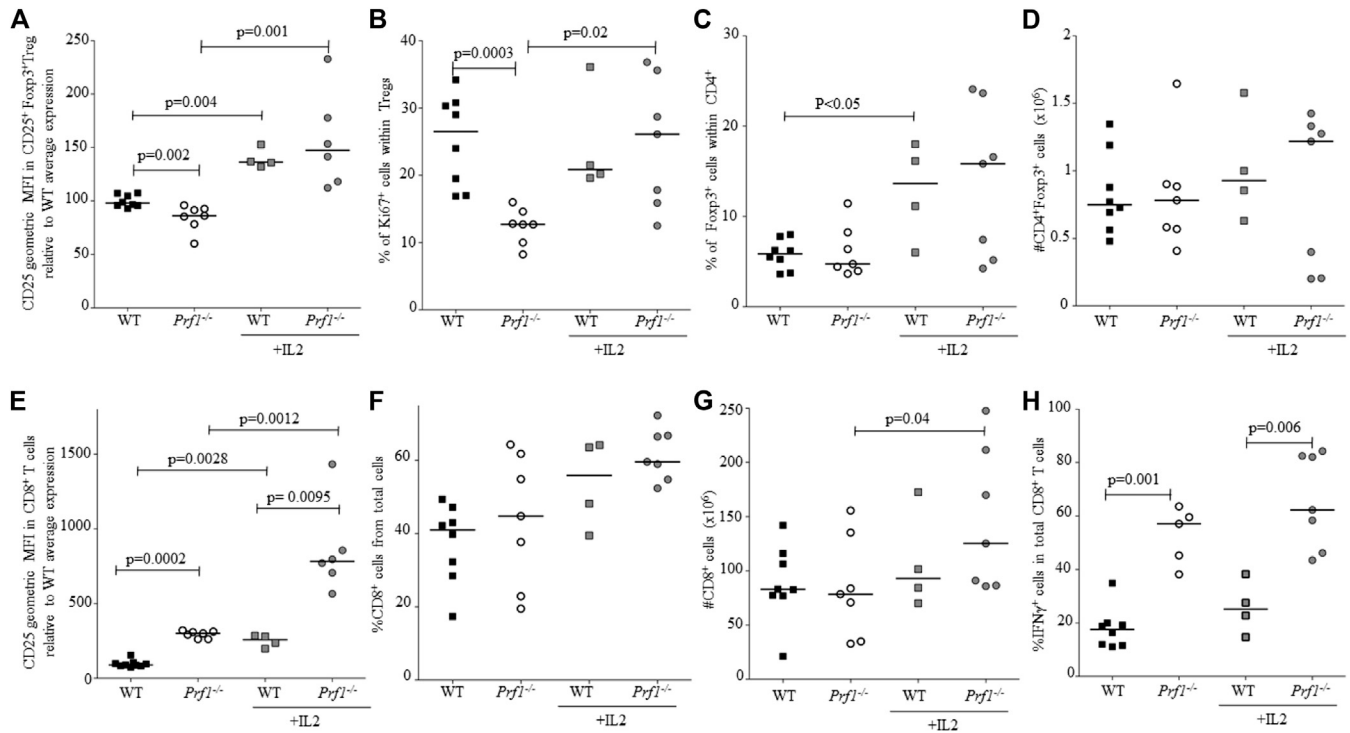
FIG E7. IL-2 elicits a feed-forward inflammatory loop during LCMV-triggered disease. Wild-type and *Prf1*^{−/−} mice and *Prf1*^{−/−} mice with or without IL-2 complex treatment were infected with LCMV-Armstrong. **A-D,** Splenic Treg cell counts were assessed (day 8) for CD25 geometric mean fluorescence intensity within CD25^{+} cells (Fig E7, *A*), Ki67 expression (Fig E7, *B*), and percentage within CD4^{+} T cells (Fig E7, *C*) and absolute number (Fig E7, *D*). **E-H,** Splenic CD8^{+} T cells were assessed for CD25 geometric mean fluorescence intensity (Fig E7, *E*), percentage within lymphocytes (Fig E7, *F*), absolute number (Fig E7, *G*), and IFN-γ expression (Fig E7, *H*). *MFI,* Mean fluorescence intensity. Medians and individual data points are shown pooled from 3 experiments.

TABLE E1. Patients' characteristics

	Diagnosis	Underlying disease	Age	Sex	Prior treatment	HLH treatment
1	MAS	sJIA	11 mo	Male	—	Corticosteroids
2	MAS	sJIA	19 y	Male	Tocilizumab	Corticosteroids
3	EBV-triggered FHL	XLP (SAP deficiency)	10 mo	Male	—	Corticosteroids and CyA
4	MAS	sJIA	14 y	Male	—	Corticosteroids*
5	EBV-induced MAS	sJIA	21 y	Male	Tocilizumab	—
6	MAS	sJIA	13 y	Female	—	—
7	FHL	FHL (*MUNC13-4* mutation)	15 mo	Male	—	—

CyA, Cyclosporine; *sJIA*, systemic juvenile idiopathic arthritis; *XLP*, X-linked lymphoproliferative syndrome.
*Patient death during episode.